A Novel Calibration Technique for Electro-Optical Proximity Sensors

A. Bonen
Department of Electrical and Computer Engineering

R. E. Saad
Department of Electrical and Computer Engineering

K. C. Smith
Department of Electrical and Computer Engineering

B. Benhabib
Department of Mechanical Engineering

Computer Integrated Manufacturing Laboratory, Department of Mechanical Engineering, University of Toronto
5 King's College Road, Toronto, Ontario, M5S 1A4 Canada, Email: beno@me.utoronto.ca

Abstract – **A novel calibration-per-group-of-surfaces methodology is proposed, by which to address the problem of surface-robustness for amplitude-modulation-based electro-optical proximity sensors. The pose-estimation polynomials produced by this calibration method provide accurate pose estimations for all the surfaces considered apriori by the calibration. Moreover, the same polynomials can be used to provide acceptable pose estimations for object surfaces not considered in the calibration. A robotic proximity sensor that comprises an electro-optical transducer and a practical electronic interface circuit is utilized for verifying the proposed methodology. Experimental results for this sensor, using a variety of surfaces and materials, are presented and discussed.**

I. INTRODUCTION

Proximity sensors, measuring the position and orientation (pose) of an object relative to a robot gripper, are needed in order to bridge the uncertainty gap between the gross proximity-estimation of a vision system and the direct contact required for tactile sensing [1,2]. The range of the proximity sensor must be sufficiently large to compensate for possible errors of the vision system, while the "approach" accuracy must permit effective grasping of the object.

Many types of proximity sensors have been built; they employ various transduction media including sound, magnetic field, electric field, and light. Presently, the electro-optical approach is the most appropriate due to: the relatively small size of the sensor, its relatively large range of operation, and the fact that almost no restrictions are imposed on the object's material.

Conventionally, electro-optical proximity sensors have utilized one of two methods of operation: the triangulation principle, or the amplitude- or phase-modulation of light intensity. For various reasons (including the smaller size of the sensor and the lack of moving parts), amplitude- modulation (AM) or phase-modulation (PM) schemes are more suited for mounting on a gripper, and thus are more commonly used. However, due to the lack of robustness of AM and PM sensors to surface-reflectance characteristics, calibration of these sensors was until now restricted to the calibration-per-surface (CPS) approach.

In this paper, a new methodology is proposed for the calibration of AM and PM sensors via a calibration-per-group-of-surfaces (CPG) technique, Section IV. As a preamble to the presentation of this methodology, the problem of robustness to surface characteristics is first described in Section II. Electro-optical transduction characteristics and the key features required from AM and PM transducers for CPG utilization are then described in Section III. The paper also provides experimental results for the implementation of CPG on an AM sensor.

II. ROBUSTNESS TO SURFACE CHARACTERISTICS

The most serious problem related to AM and PM sensors is their susceptibility to variations in the reflectivity characteristics of objects' surfaces. This problem is rarely addressed in the literature, and even when it is considered, the proposed approaches are quite limited. They generally include optimization of the robustness of the sensor to surface characteristics via the geometrical design of the sensor [3], or construction of a calibration-per-surface database, and thereby making use of apriori knowledge in order to pick appropriate calibration-information [4-6].

A truly adaptive and robust system, however, cannot rely on the above-mentioned solutions. Accuracy achieved using optimization via geometrical design would be far lower than the accuracy needed from such sensors. As for the alternative approach, namely building a large data-base of calibration information for each of the possible surfaces, it is costly in initial setup time. Furthermore, the data-base must be updated with the results of a new calibration process, every time a new object is added to the object-set handled by the robot.

A unique approach to improving upon the accuracy and robustness of such proximity sensors is described herein. Although in principle, an AM transducer with one emitter and three receivers is sufficient for extracting the required 3D information, a transducer with eight receivers is considered here. Similarly, instead of the minimal PM-transducer requirement of two emitters and three receivers, a transducer with four emitters and five receivers is proposed. The information provided by the "redundant" reflection measurements is used in the calibration process to produce a pose estimation that minimizes the dependency on surface-reflection characteristics. This issue is further discussed in Section IV.

III. ELECTRO-OPTICAL TRANSDUCTION

A. Light Reflection

One of two different approaches is usually followed in describing optics in general, and reflection in particular: (i) the physical approach, based directly on wave theory and Maxwell's equations [7]; and, (ii) the geometrical approach, which uses a simplifying approximation [8].

0-7803-3026-9/95 $4.00 © 1995 IEEE

Several mechanisms are involved in producing the reflectance pattern of a surface, resulting in three components: the specular spike, the specular lobe, and the diffused lobe (Fig. 1). The specular spike is produced by very smooth (mirror-like) surfaces. In the manufacturing environment such spikes will exist in reflections from polished and coated surfaces. The specular lobe is produced by a (random) distribution of micro-planes whose dimensions are greater than the optical wavelength but much smaller than the beam width. This reflection is typical for roughly-ground objects.

The diffused lobe originates from diffraction, either from very rough surfaces with a small correlation distance, or from internal refraction. Because of the high conductivity of metal surfaces, most of the light reflects from the interface between the metal and the air, while the portion that penetrates into the metal surface is absorbed. Accordingly, the reflection intensity originating from internal refraction in metal is practically zero. In dielectrics however, a large portion of the light penetrates into the surface, and then reflects back out as diffused light.

B. Phase-Modulated Transduction

A PM proximity transducer usually consists of two light sources and one or more photodetectors [6,9]. The light sources are driven by modulated sinusoidal signals having a 90° phase relationship (Fig. 2).

The emitter control-voltages, V_{em1} and V_{em2}, have amplitudes of a and b respectively:

$$V_{em1}(t)=a\cdot\cos\omega t\,, \tag{1}$$

$$V_{em2}(t)=b\cdot\sin\omega t\,. \tag{2}$$

The detected signal is a superposition of the two reflected signals, having corresponding attenuations of A and B.

$$V_{rec}(t)=A\cdot V_{em1}+B\cdot V_{em2}\,. \tag{3}$$

The signal attenuation is a function of the geometrical and electrical parameters of the sensor, the reflectivity characteristics of the object's surface, and the surface's distance and orientation with respect to the sensor. The combined signal at the receiver is therefore:

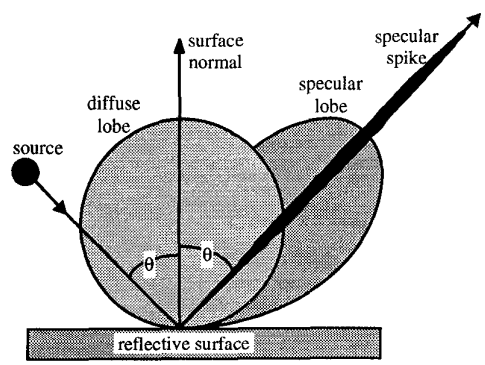

Fig. 1. Three types of reflection.

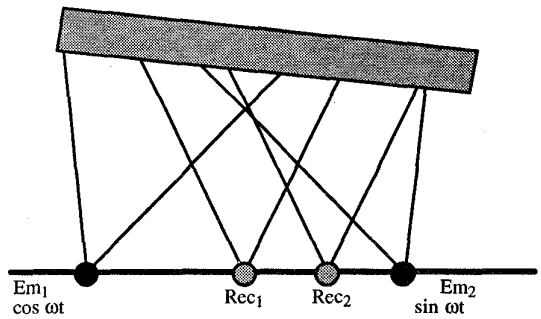

Fig. 2. A phase-modulated proximity sensor.

$$V_{rec}(t)=C\cdot\sin(\omega t+\varphi)\,, \tag{4}$$

where C is the combined attenuation-function, and φ is the combined phase-shift.

Usually only the phase information φ is used, and the amplitude is completely neglected or used only for verifying the likelihood of error and estimating its magnitude.

It can also be noted that, in general, orientation-sensing requires symmetry, while distance-sensing requires asymmetry in the configuration of the emitters. Light originates concurrently from two emitters that are positioned symmetrically in relation to a virtual point. The position of the receiver at or beside this point arranges either a symmetrical or an asymmetrical configuration. The two receivers of the basic PM proximity sensor in Fig. 2 can therefore be used for measuring both distance and orientation: Rec_1 can be used for orientation measurement, while Rec_2 is suited for distance measurement.

C. Amplitude-Modulated Transduction

An AM transducer usually consists of one emitter and several receivers (Fig. 3). The signal amplitude at each detector is a function of all the sensor's geometrical parameters, the reflectivity characteristics of the object's surface, and its pose. Thus, the surface pose can be deduced when sufficient knowledge exists about the other parameters. In any measurement, at least two detectors are used in order to compensate for changes in various parameters such as light-source intensity, and surface reflectivity [3,4]. Typical output curves of an AM sensor are shown in Fig. 4.

The symmetry property applies also to AM transducers: orientation-sensing requires symmetry, while distance-

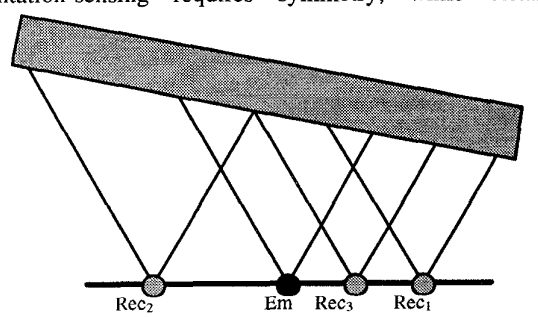

Fig. 3. An amplitude-modulated proximity sensor.

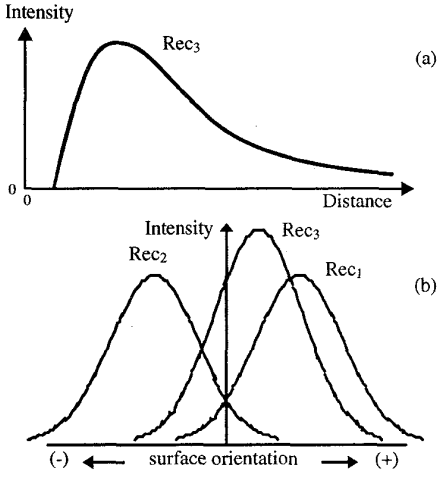

Fig. 4. The light intensity detected as a function of (a) distance, (b) orientation.

sensing requires asymmetry. However, in AM transducers the receivers rather than the emitters are paired. The three receivers of the basic AM proximity sensor in Fig. 3 can therefore be used for measuring both distance and orientation: the pair Rec_1-Rec_2 can be used for orientation measurement, while the pair Rec_1-Rec_3 is suited for distance measurement.

AM sensors can be configured such that their accuracy will increase as the robot gripper nears the contact point, at which both the orientation and the distance are zero [4,5]. In the case of distance measurement, the sensitivity and accuracy of the sensor is inversely related to the distance squared.

D. The Experimental Transducer

The transducer presented in this section combines features of both basic distance and orientation transducers. It is thus capable of measuring the distance and two-dimensional orientation of an object's surface in both the AM and PM schemes.

For the PM-scheme, the transducer can have four emitters and five receivers, Fig. 5a. The measurement of distance and two-degree-of-freedom orientation requires two stages. During the first stage, the Emitter-Pair 1-3 with Receiver 5 can be used to measure horizontal-orientation, and Receivers 1 and 3 can each supply a distance measurement. During the second stage the Emitter-Pair 2-4 with Receiver 5 can be used to measure vertical-orientation, and Receivers 2 and 4 can each supply a distance measurement. In practice, however, all five receivers should be utilized during each stage in order to supply the required measurement redundancy. Other configurations of receivers and emitters are possible as well.

For the AM-scheme, the transducer can have a single emitter and eight receivers, Fig. 5b. The measurement requires a single stage, during which all eight receivers are utilized.

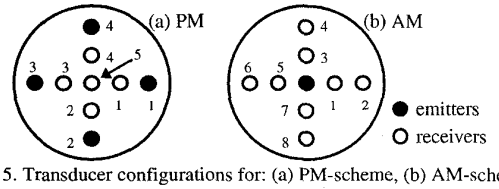

Fig. 5. Transducer configurations for: (a) PM-scheme, (b) AM-scheme.

An experimental transducer was designed and built to be capable of measuring a distance range of 40mm, and two-degree-of-freedom orientation equivalent to an overall inclination of up to ±30°. Fiber-optic-cables were used to facilitate the operation of sensitive low-noise circuitry in a shielded environment appropriately remote from any electro-magnetic-interference sources. The transducer's geometrical design was optimized with respect to sensitivity and accuracy of the required measurements, Fig. 6.

IV. SENSOR CALIBRATION METHODOLOGY

A. The Model

Several different calibration approaches were attempted in an effort to find the one that best suits the CPG scheme. The results from a "black-box" type approach of symmetrical-polynomial fit proved to be superior to all others. The term "symmetrical-polynomial" indicates that the polynomial possesses both positive and negative powers of the variables. The general form of the polynomial relationship utilized for the calibration can be expressed as follows:

$$g = \sum_{i=1}^{N} c_i \cdot h_i , \qquad (5)$$

where g is the individual estimated parameter, h_i is the ith input parameter, and c_i is the coefficient associated with the ith parameter. Herein, the parameter (polynomial element) h_i is calculated from the measured light intensities (AM), or phase shifts (PM) as follows:

$$h_i = \prod_{j=1}^{n_f} l_j^{\,p_{ij}} , \quad \forall i \quad \sum_{j=1}^{n_f} |p_{ij}| \le r , \quad |p_{ij}| \in \{0,1,2,\cdots\} , \qquad (6)$$

where l_j is one of the n_f light intensities (AM), or phase shifts (PM) supplied by the transducer, p_{ij} is the power of the signal l_j, and r is the order of the polynomial.

The output of the calibration process is a vector of constants associated with the above elements. Three such vectors are produced to construct three polynomials for the

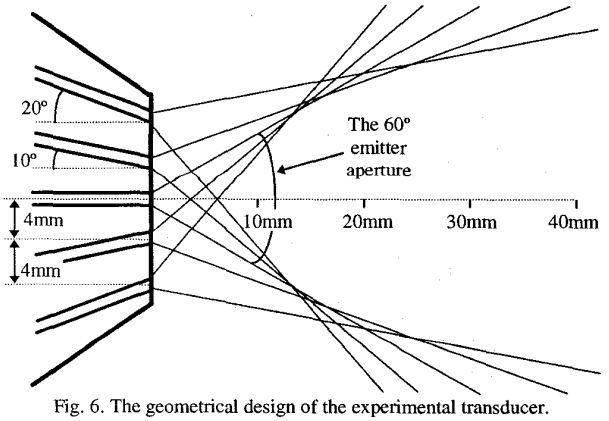

Fig. 6. The geometrical design of the experimental transducer.

individual estimation of x, u, and v (distance, horizontal orientation and vertical orientation).

The accuracy of the estimation polynomial would naturally rise with the value of r. However, the number of polynomial elements would rise significantly as well, and so would the associated computation cost in off-line calculation of the polynomial's coefficients, and for real-time pose estimation. In our work, the best accuracy-versus-cost performance tradeoff was achieved with r=3 for all the three polynomials.

B. Calibration Sub-Regions

One problem related to the use of the calibration model discussed above is the low achievable accuracy when attempting to calibrate the proximity sensor over its complete intended operating range. Over this range there exist extensive variations in the light-intensities measured by the eight receivers. Moreover, this type of calibration does not take advantage of the available increased accuracy as the gripper nears the contact point.

Thus, the accuracy of the calibration can be greatly improved by dividing the 3D operation range into sub-regions. Using this approach, the calibration process supplies different polynomials for the different sub-regions. An empirically-determined specific set of four overlapping sub-regions: "wide", "medium", "narrow", and "fine" was selected for the calibration of our proximity sensor, (Fig. 7).

Utilization of a multi-region-calibration scheme, however, adds another stage to the 3D-pose-estimation algorithm. While in the case of a single calibration region only a single polynomial is needed for estimation, in the multi-region case four separate estimations can be made by the four different polynomials. One of two approaches can then be followed:

1. The four estimations can be calculated with a reliability factor attached to each one. The reliability factor can be calculated from the relation between the estimated pose and the sub-region's boundaries. Thereafter, the four estimations can be treated by a sensor-fusion technique as if they were created by different sensors, and the most reliable estimation can be determined.
2. Both the complete-region and multi-region calibrations can be utilized. The low-accuracy pose estimated by the complete-region calibration can be used to indicate which of the sub-region polynomials should be used for the more accurate estimation.

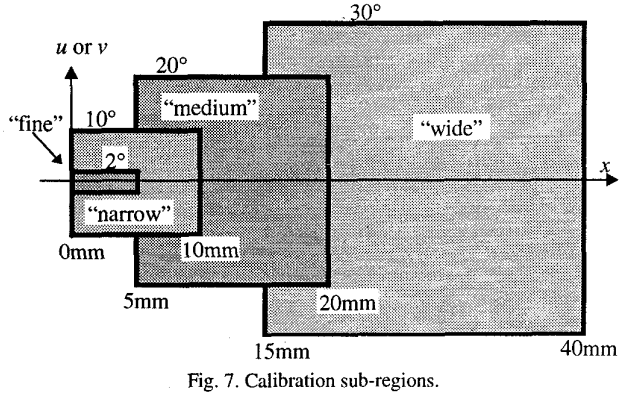

Fig. 7. Calibration sub-regions.

C. Calibration per Group of Surfaces

Creation of pose-estimation polynomials using a calibration-per-surface (CPS) approach is a simple process. This approach would yield very accurate estimations when the sensor is used for the specific surfaces utilized during calibration. However, as noted in Section II, even besides being surface-specific, the CPS approach is very vulnerable to variations in the surface reflection characteristics. The accuracy achieved by CPS can decrease rapidly due to lack of uniformity in surface detail, and variations in the surface roughness of objects which are made of the same material. Moreover, CPS requires the existence of an apriori knowledge of the surface identity. Thus, the CPS technique is not a practical technique for manufacturing environments.

Accordingly, a calibration-per-group (CPG) technique is proposed herein to address the above robustness problems. Within the framework of this approach, a global relationship is derived for the input/output of the sensor by grouping object-specific data obtained during the calibration process. A group can be composed of a collection of surfaces made of the same material but with different surface-roughnesses, or surfaces made of different materials but with similar surface-related reflection characteristics.

Although the CPG technique is less accurate than the CPS technique for any specific surface utilized during the calibration, it can provide very-comparable estimations as the relative pose of the surface gets smaller. Also, unlike the CPS technique, the CPG technique involves a variety of materials and surface roughnesses. Thus, it can provide acceptable pose estimations for objects that were not included in the original calibration group, but which have similar reflection properties to that of the group.

VI. EXPERIMENTATION

A. Experimental Setup

The performance of optical transducers is in general limited by their electronic interfaces. Thus, a robust and reliable computer-interface was developed for the AM implementation of our proximity transducer. The interface comprises a circuit with one transmitter and eight receivers, built on a PC I/O card, in conjunction with a commercially-available controller card (Fig. 8) [10].

Through our interface circuit, optical-noise interference is reduced to less than a measurable level, even in extremely bright "light-infested" surroundings, by utilizing a modulated laser-diode together with optical and electrical filtering.

The interface circuit also significantly increases the dynamic range of the proximity sensor. The power of the

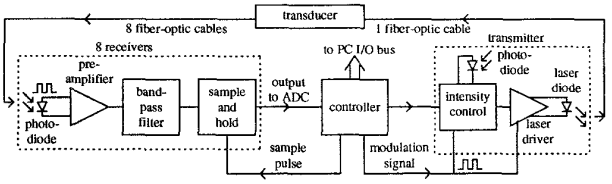

Fig. 8. Proximity-sensor block diagram.

light-source is monitored in a dynamic intensity-control loop designed to perform "floating-point" measurements according to the attenuation found in the associated optical path. By this means, the sensor acquires the combined dynamic ranges of the receiver and transmitter circuits.

The performance of the new interface design was investigated through an analysis of its signal characteristics (including frequency response, noise, sensitivity, dynamic range, and time-domain performance). The results obtained include a receiver dynamic range of 62dB and an overall dynamic range of 134dB (when the minimum SNR is taken to be 10dB), a receiver input noise of $1.52\text{pA}/\sqrt{\text{Hz}}$, and operating-frequency range of 0.5kHz to 135kHz.

In our experimental setup, the object surface was mounted on a 3-degree-of-freedom numerically-controlled optical precision table, while the position of the proximity transducer was fixed. Through the use of the setup, a fully-automatic control was established over the movement of the object-surface, as well as over the measurement-acquisition process.

B. Calibration Results

Experiments were conducted to compare the accuracy achieved by the CPG and CPS methods using various materials. Individual CPS calibrations were first carried out for aluminum, copper, brass, stainless-steel, teflon, PVC, wood, and plexiglas surfaces. These materials were then classified into two separate groups, namely metals and dielectrics, and CPG calibrations were conducted on these groups. Finally, all the materials were combined into a single group and an overall general calibration (GC) was obtained.

The calibration measurements for x, u, and v were acquired at selected points in a three-dimensional variable space. A set of 1,960 pre-determined points was used to obtain measurements from all the surfaces considered. The points were selected according to a special distribution function designed to achieve better accuracy when the orientation and the distance of the surface are closer to zero.

Results were analyzed with respect to the calculated estimation-errors. The calibration-error for a given measurement is defined herein as the difference between the known pose of the surface, where the measurement was taken, and the pose estimated by utilizing the calibration polynomials. By way of an example, the means (μ) and standard deviations (σ) of the estimation-errors of the distance (x) and vertical-orientation (u) are given in Table 1 for the fine region (the horizontal-orientation results are very similar to those of the vertical-orientation). In the case of group calibrations, also given are the results of the combined standard deviations for all the materials within the group (namely for all dielectrics, all metals, and all materials).

TABLE 1. ESTIMATION-ERRORS' $\mu\pm\sigma$ IN THE FINE REGION.

variable	$\mu_x\pm\sigma_x$(mm)			$\mu_u\pm\sigma_u$(°)		
method	CPS	CPG	GC	CPS	CPG	GC
aluminum	0±0.009	0±0.020	-0.001±0.044	0±0.015	0±0.022	0±0.056
brass	0±0.010	0±0.018	0±0.028	0±0.015	0±0.019	0±0.050
copper	0±0.007	0±0.021	0.001±0.041	0±0.015	0±0.022	-0.001±0.057
st. steel	0±0.010	0±0.023	-0.001±0.038	0±0.017	0±0.025	-0.001±0.072
pvc	0±0.004	0±0.004	0±0.021	0±0.023	0±0.025	0±0.041
plexiglas	0±0.003	0±0.006	0±0.020	0±0.016	0±0.024	0±0.035
teflon	0±0.003	0±0.006	0.001±0.029	0±0.025	0±0.030	0±0.046
wood	0±0.004	0±0.006	0±0.036	0±0.038	0±0.043	0.001±0.073
metals	N/A	0±0.021	N/A	N/A	0±0.022	N/A
dielectrics	N/A	0±0.005	N/A	N/A	0±0.032	N/A
general	N/A	N/A	0±0.033	N/A	N/A	0±0.055

A comprehensive summary of the CPS, CPG and GC calibrations for all regions and materials is also given herein in Table 2. The entries in this table represent the average value of ($|\mu|+\sigma$) normalized with respect to the best-estimation value encountered (that is, CPS fine ≡ 1). The normalization factors were: 0.00625mm for x, 0.0205° for u, and 0.01625° for v.

The following three points summarize our observations:

1. The estimation-errors decrease significantly as the measurement regions become smaller and nearer to the transducer.
2. The estimation-errors of the CPS technique are smaller than those of both the CPG and GC techniques. However, the differences are significantly smaller for the "fine" sub-region, where (in absolute terms) they may be negligible.
3. The estimation-errors of the CPG technique are smaller than those of the GC technique.

Naturally, the means of the estimation-errors are around zero as long as they are calculated for 100% of the population. However, a small bias is displayed in GC estimations by population subsets, which are composed of the samples of a single surface. This bias is a measure of the uniformity of reflection characteristics inside a group, and particularly, a measure of how far the reflection characteristics of a surface deviate from the group's average. Thus, this property may

TABLE 2. NORMALIZED ACCURACIES OF THE CALIBRATION RESULTS.

variable	x (× 0.00625mm)			u (× 0.0205°)			v (× 0.01625°)		
method	CPS	CPG	GC	CPS	CPG	GC	CPS	CPG	GC
fine	1.0	2.1	5.2	1.0	1.3	2.6	1.0	1.4	3.4
narrow	1.7	14.8	46.1	1.6	3.8	27.1	1.5	5.8	27.4
medium	5.1	115	282	3.3	18.9	84.9	3.4	29.4	123
wide	28.6	347	620	9.6	72.2	201	11.5	92.7	245
complete	32.1	426	796	11.8	88.0	225	12.1	101	297

assist in the categorization of surfaces into groups.

The validity of the observed results was verified as follows: Additional and independent random samples sets of 70 measurements were obtained, for every material and sub-region, at different poses than those used for the calibration. Again, the estimation-errors were analyzed. Both the means and standard deviations of the samples' errors were within the statistical limits calculated from the basic calibration results according to Sampling Theory [11].

C. Uncalibrated Surfaces

This section explores the possibility of using the CPG-scheme calibration for pose estimations on surfaces that are not included in the original group. Experiments were conducted with two *new* materials (galvanized steel and white paper), and with an aluminum sample (aluminum-2) having a surface-roughness different than the one used in the previous experiments. Measurement points obtained for these materials were gathered with the same distribution parameters used in the previous experiments (1,960 points).

By way of an example, the estimation-errors' means and standard deviations for the fine region are given in Table 3. Estimation errors in other regions display the same relative accuracies as given in Table 2. The results can be used to compare the performance of the GC, CPG-metals, CPG-dielectrics, and CPS-aluminum with respect to the new materials.

The following two points summarize our observations:

1. The estimations of CPG/CG can permit effective pose-estimation of uncalibrated surfaces.
2. In the case of the same material but a different surface-roughness, the estimation accuracies of CPG/CG are better than these of the CPS technique.

CONCLUSION

A new methodology, calibration-per-group of surfaces (CPG), was employed in an attempt to address the problem of robustness of electro-optical proximity sensors to surface-reflection characteristics. The features of AM and PM transducers required for the implementation of this method were discussed. As an example, a transducer that allows the utilization of this methodology in both the AM and PM schemes was presented.

The results of experiments that utilized an experimental transducer in an AM scheme were given. The sensor was calibrated individually for eight different materials using CPS, as well as globally for all eight materials and for two groups of materials (metals and dielectrics) using CPG. Physical experiments verified the expected good performance of the CPG-calibrated proximity sensor for all the apriori considered surfaces, as well as for surfaces not considered apriori.

TABLE 3. ESTIMATION-ERRORS' $\mu\pm\sigma$ IN THE FINE REGION FOR UNCALIBRATED SURFACES.

variable	method	galvanized steel	white paper	aluminum-2
$\mu_x\pm\sigma_x$(mm)	GC	-0.21±0.31	0.53±0.45	0.59±0.26
	CPG - metals	-0.07±0.24	2.96±1.47	0.92±0.19
	CPG - dielectrics	—[1]	0.20±0.25	—
	CPS - aluminum	N/A	N/A	(-1.43±3.78)
$\mu_u\pm\sigma_u$(°)	GC	0.09±0.58	-3.42±0.63	-0.41±0.51
	CPG - metals	-0.38±0.24	-2.52±5.10	-0.71±0.22
	CPG - dielectrics	—	-3.77±1.14	—
	CPS - aluminum	N/A	N/A	(8.63±10.7)
$\mu_v\pm\sigma_v$(°)	GC	0.34±0.64	1.89±0.29	0.12±0.45
	CPG - metals	-0.48±0.41	-0.27±1.34	-0.23±0.28
	CPG - dielectrics	—	1.26±0.54	—
	CPS - aluminum	N/A	N/A	(7.34±4.13)

ACKNOWLEDGMENT

We gratefully acknowledge the financial support of the Natural Sciences and Engineering Research Council of Canada.

REFERENCES

[1] B. Espiau, "An overview of local environment sensing in robotics applications," *Sensors and Sensory Systems for Advanced Robots, NATO ASI Series* Vol. F43, pp. 125-151, Berlin, 1988.

[2] A. Bradshaw, "Sensors for mobile robots," *Measurement and Control*, Vol. 23, No. 2, pp. 48-52, March 1990.

[3] P. P. L. Regtien, "Accurate optical proximity detector," *IEEE Conf. on Instrumentation and Measurement Technology*, pp. 141-143, San Jose, CA, Feb. 1990.

[4] O. Partaatmadja, B. Benhabib, E. Kaizerman and M.Q. Dai, "A two-dimentional orientation sensor," *Journal of Robotic Systems*, Vol. 9, No. 3, pp. 365-383, 1992.

[5] O. Partaatmadja, B. Benhabib and A.A. Goldenberg, "Analysis and design of a robotic distance sensor," *Journal of Robotic Systems*, Vol. 10, No. 4, pp. 427-445, June 1993.

[6] H. Kopola, S. Nissilä, R. Myllylä and P. Kärkkäinen, "Intensity modulated fiber optic sensors for robot feedback control in precision assembly," *SPIE, Fiber Optic Sensors II*, Vol. 798, pp. 166-175, Hague, The Netherlands, March 1987.

[7] P. Beckmann and A. Spizzichino, *The Scattering of Electromagnetic Waves from Rough Surfaces*, Pergamon press, New York, 1963.

[8] K. Torrance and E. Sparrow, "Theory for off-specular reflection from roughened surfaces," *Journal of the Optical Society of America*, Vol. 57, pp. 1105-1114, Sep. 1967.

[9] R. Masuda, "Multifunctional optical proximity sensor using phase modulation," *Journal of Robotic Systems*, Vol. 3, No. 2, pp. 137-147, 1986.

[10] A. Bonen, R. E. Saad, B. Benhabib and K.C. Smith, "A novel opto-electronics interface-circuit design for sensing applications," *IEEE, Conf. on Instrumentation and Measurement Technology*, pp. 658-663, Boston, Mass., April 1995.

[11] R. E. Walpole and R. H. Myers, *Probability and Statistics for Engineers and Scientists*, 5th Edition, Macmillan Publishing Company, 1993.

1 Results with ($|\mu|\pm\sigma$) values larger than the region's span (e.g., 5mm and 4° in the fine region herein) are replaced with the symbol "—", or given in brackets.